

Precision on the top mass

Stefan Weinzierl

*PRISMA Cluster of Excellence, Institut für Physik, Johannes Gutenberg-Universität Mainz,
D - 55099 Mainz, Germany*

In this talk I will focus on theoretical issues related to high precision determinations of the top mass. Several mass definitions are reviewed and their respective advantages and disadvantages are discussed. Precision determinations of the top mass will require a short-distance mass definition. I will summarise current work in this direction.

1 Introduction

The top quark mass – or equivalently the top Yukawa coupling – is one of the fundamental parameters of the Standard Model. Precise values for these fundamental parameters encode our current knowledge of the Standard Model and are required for various reasons. Focusing on the top quark mass, the motivations for a precision determination are as follows: First of all, the value of the top mass affects the theory predictions for top quark cross sections. It is therefore relevant in comparing measured top quark cross sections from the Tevatron and the ongoing LHC experiments with theoretical predictions of the Standard Model. Secondly, the value of the top mass affects searches for new particles in beyond the Standard Model (BSM) scenarios. Examples are searches for processes with top background or BSM decays into top quarks. For these first two reasons it is desirable to determine the top quark mass at least to a precision, such that the error originating from the top quark mass is not dominating the final error of the analysis. Currently, this would call for a high precision on the value of the top mass, but not for a very high precision. However, there are also reasons why a very high precision is desirable: The top quark mass is close to the electro-weak symmetry breaking scale $v = 246$ GeV. If there is new physics associated with electro-weak symmetry breaking, top quark physics is a place to look for. New particles with masses above energies accessible with current collider experiments may nevertheless leave their traces in quantum corrections. Therefore the combination of experimental precision measurements and theoretical precision calculations will be sensitive to new physics at higher scales. This is a very strong reason for a high precision determination of the top quark mass. As a final reason let us also mention, that if we assume the Standard Model to be valid to very high scales (possibly as high as the Planck scale), the stability of the electro-weak vacuum crucially depends on the precise numerical value of the top quark mass.

Let me also say from the very beginning that although I used the colloquial phrase “the top quark mass”, there is nothing like “the” top quark mass. Like any other parameter in the Lagrangian of the Standard Model, the top quark mass will be subject to renormalisation. Like any other renormalised quantity, the renormalised top quark mass will depend on a chosen renormalisation scheme. As there are several possible renormalisation schemes, there is more than one legitimate definition of a renormalised top quark mass. In this talk I will discuss

subtleties of some popular mass renormalisation schemes and the way they affect experimental measurements.

2 Basic facts about the top quark

The top quark is the heaviest elementary particle known up to today. It has been discovered twenty years ago at the Tevatron^{1,2} and it is currently studied at the LHC. The physics of the top quark is governed to a large extent by two essential numbers, the top quark mass and the top quark width. The current values of the top mass and the top width are^{3,4}

$$m_t = 173.21 \pm 0.51 \pm 0.71 \text{ GeV}, \quad \Gamma_t = 2.1 \pm 0.5 \text{ GeV}. \quad (1)$$

With a mass of roughly 173 GeV the top quark is heavier than all other known elementary particles. This large mass sets also a hard scale. From the top quark width one deduces immediately that the top quark lifetime ($\tau_t = \hbar/\Gamma_t$) is shorter than the characteristic hadronisation time scale. This implies that the top quark decays before it can form bound states. Given the facts that the large top quark mass sets a hard scale and that top quarks do not hadronise it follows that top quark physics is an ideal place for the application of perturbative QCD.

On the other hand it should not be forgotten that the top quark is like any other quark a colour-charged particle. Furthermore, the top quark is like any other quark of the second or third generation an unstable particle. These two facts imply that there is no asymptotic free top quark state in quantum field theory. Although top quark physics is described mainly by perturbative QCD, one has to pay attention that non-perturbative effects – originating from the fact that one deals with coloured and/or unstable particles – do not enter from the back door.

A characteristic scale of non-perturbative effects is Λ_{QCD} . We can see from eq. (1) that the error on the top quark mass is approaching $\mathcal{O}(\Lambda_{\text{QCD}})$. This raises immediately the question if the top quark mass can be measured with a precision better than $\mathcal{O}(\Lambda_{\text{QCD}})$. Of course, the top quark mass is determined from experimental measurements and it seems at first sight that reducing the error would just imply improving the experimental precision. However, this is not the full story. Up to now there is no “theory-free” experimental determination of the top quark mass. Experimental measurements of the top quark mass rely on theoretical input for example through the template method or the matrix element method. In this way theoretical uncertainties might enter the determination of the top quark mass. There are now two possible scenarios, depending on the chosen mass definition. In the first – and not so favourable – scenario the extraction of the top mass is limited by non-perturbative effects of order Λ_{QCD} . This means, that the precision on the top mass cannot be improved beyond $\mathcal{O}(\Lambda_{\text{QCD}})$ by calculating perturbative higher-order corrections. The pole mass definition is an example for this scenario. In the second – and more favourable – scenario, one is not limited by non-perturbative effects and the precision on the top mass can – at least in principle – be improved below $\mathcal{O}(\Lambda_{\text{QCD}})$ by the inclusion of perturbative higher-order corrections. Short-distance mass definitions are examples of the second scenario.

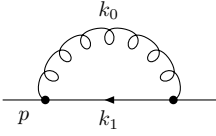
3 Basic facts about a fermion mass

Let us now review the advantages and disadvantages of several mass definitions. The starting point for a theoretical description is the Lagrange density, the relevant part reads

$$\mathcal{L}_{\text{fermion}} = \bar{\psi}_{\text{bare}} (i \not{D} - m_{\text{bare}}) \psi_{\text{bare}}. \quad (2)$$

Beyond leading-order in perturbation theory loop diagrams have to be taken into account. One of the simplest loop diagrams, which nevertheless allows us to discuss all relevant features, is

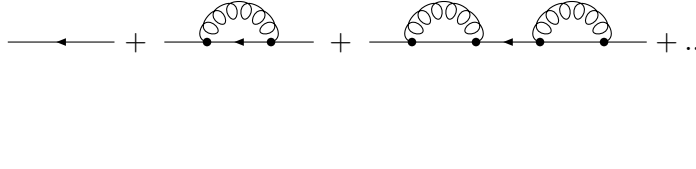
the one-loop fermion self-energy:

$$-i\Sigma = \text{diagram} = \frac{g^2 C_F}{\mu^{D-4}} \int \frac{d^D k}{(2\pi)^D} i\gamma_\rho \frac{i}{\not{k}_1 - m_{\text{bare}}} i\gamma^\rho \frac{(-i)}{k_0^2}. \quad (3)$$


In four space-time dimensions the loop integral is divergent. A convenient method of regularisation is the continuation of the number of space-time dimensions to $D = 4 - 2\varepsilon$, the divergences will then show up as poles $1/\varepsilon$. Within dimensional regularisation one introduces in addition an arbitrary scale μ in order to keep the mass dimension of the regulated expression to its four-dimensional value. The loop integral in eq. (3) is easily computed and the result has with respect to the spinor structure the form

$$-i\Sigma = -i(A\not{p} + Bm_{\text{bare}}). \quad (4)$$

Here, A and B are functions of p^2 , m_{bare}^2 , μ^2 and ε . As a function of ε , the quantities A and B have a Laurent series expansion in ε starting with ε^{-1} . Iterations of self-energy insertions may be resummed similar to the resummation of a geometric series:

$$\begin{aligned} \text{diagram} + \text{diagram} + \text{diagram} + \dots &= \frac{i}{\not{p} - m_{\text{bare}} - \Sigma} \\ &= \frac{i(1+A)}{\not{p} - (1+A+B)m_{\text{bare}}} + \mathcal{O}(\alpha_s^2). \end{aligned} \quad (5)$$


Renormalisation relates the bare quantities to the renormalised quantities. We have to consider the quark field renormalisation and the mass renormalisation:

$$\psi_{\text{bare}} = \sqrt{Z_2} \psi_{\text{renorm}}, \quad m_{\text{bare}} = Z_m m_{\text{renorm}}. \quad (6)$$

The quark field renormalisation allows us to absorb the divergences of the expression $(1+A)$ in the numerator of eq. (5) into Z_2 , the mass renormalisation allows us to absorb the divergences of $(1+A+B)$ in the denominator of eq. (5) into Z_m . It should be stressed that the renormalisation constants and hence the renormalised quantities depend on the renormalisation scheme. In particular, the renormalised mass m_{renorm} depends on the renormalisation scheme. All renormalisation schemes entail that they absorb the ultraviolet divergent terms. Different renormalisation schemes differ in additional non-ultraviolet divergent terms.

4 Implications on the precision for the top quark mass

Let us now review different mass renormalisation schemes and its implications on the determination of the renormalised top quark mass in a given scheme.

4.1 The $\overline{\text{MS}}$ -scheme

The $\overline{\text{MS}}$ -scheme absorbs by definition only the parts proportional to $\frac{1}{\varepsilon} - \gamma_E + \ln(4\pi)$ and nothing else into the renormalisation constant Z_m . The renormalised and resummed quark propagator of eq. (5) reads then

$$\frac{i}{\not{p} - m_{\overline{\text{MS}}} - (A+B)_{\text{fin}} m_{\overline{\text{MS}}}} \quad (7)$$

The essential properties of the $\overline{\text{MS}}$ -mass can already be deduced from eq. (7): Although not indicated explicitly, the $\overline{\text{MS}}$ -mass depends on the scale μ , leading to the concept of a running

mass. This follows from eq. (6): The bare mass m_{bare} is of course scale-independent, while Z_m and in consequence also $m_{\overline{\text{MS}}}$ depend on μ . Secondly, the presence of the finite terms $(A+B)_{\text{fin}} m_{\overline{\text{MS}}}$ in the denominator shows, that the propagator does not have a pole at $p^2 = m_{\overline{\text{MS}}}^2$ and matrix elements do not factor at $p^2 = m_{\overline{\text{MS}}}^2$. Thirdly, the extra terms $(A+B)_{\text{fin}}$ in the denominator are not constant as a function of p^2 , they vary with p^2 . This implies that the propagator in eq. (7) will not yield a Breit-Wigner shape. These properties should be kept in mind, when performing an analysis based on the $\overline{\text{MS}}$ -mass.

The $\overline{\text{MS}}$ -mass $m_{\overline{\text{MS}}}$ is an example of a short-distance mass, meaning that the mass definition is not affected by long-distance non-perturbative effects. The $\overline{\text{MS}}$ -mass can be extracted from an infrared-safe observable^{5,6} for a process like $pp \rightarrow l\bar{\nu}jjb\bar{b}$ at high energies by comparing for example σ_{exp} with $\sigma_{\text{theo}}(m_{\overline{\text{MS}}})$. It should be stressed that the error of such a measurement is not affected by an $\mathcal{O}(\Lambda_{\text{QCD}})$ -barrier. This is related to the fact that $\overline{\text{MS}}$ -mass is a short-distance mass. On the theory side, the uncertainty can systematically be improved by the inclusion of higher-order corrections. The current state-of-the-art are NNLO calculations⁷ with NNLL resummation^{8,9,10,11,12,13} for $pp \rightarrow t\bar{t}$ and NLO calculations for the process $pp \rightarrow b\bar{b}W^+W^-$ including top decays and non-factorisable corrections^{14,15}. At present, the dominant sources for the error on the determination of the $\overline{\text{MS}}$ -mass from cross section measurements originates from uncertainties on α_s , the parton distribution functions and experimental uncertainties. None of those are specific to the chosen mass definition. A useful quantity in this context is the sensitivity \mathcal{S} defined by

$$\left| \frac{\delta\sigma}{\sigma} \right| = \mathcal{S} \left| \frac{\delta m_{\overline{\text{MS}}}}{m_{\overline{\text{MS}}}} \right|. \quad (8)$$

For the determination of the top mass from the total cross section for $t\bar{t}$ -production the sensitivity is $\mathcal{S} \approx 5$. The current error on the determination of the $\overline{\text{MS}}$ -mass $m_{\overline{\text{MS}}}$ along these lines is about 2 GeV.

As a significant fraction of $t\bar{t}$ -events actually are accompanied by additional jets, also the process $pp \rightarrow t\bar{t} + \text{jet}$ is of interest. For this process NLO calculations are available^{16,17,18,19}. Differential distributions for this process show a sensitivity in the range $\mathcal{S} \approx 10 \dots 20$ and have therefore the potential for a more precise extraction of the top mass²⁰.

4.2 The on-shell-scheme

In the on-shell scheme the mass renormalisation constant Z_m is defined in such a way that the propagator has a pole at m_{pole} , (and m_{pole} is therefore called the pole mass). The renormalised and resummed quark propagator is then by definition

$$\frac{i}{\not{p} - m_{\text{pole}}}. \quad (9)$$

The pole mass m_{pole} includes the width and is therefore a complex quantity. The pole mass has the advantage that matrix elements factor at $p^2 = m_{\text{pole}}^2$ and that the propagator of eq. (9) leads to a Breit-Wigner shape. However, there is a major disadvantage: The pole mass is not a short-distance mass and sensitive to long-distance non-perturbative effects. In the on-shell scheme, the renormalisation constant Z_m contains contributions from all momentum scales, not just the ultraviolet region. It can be shown that in higher order in perturbation theory subsets of diagrams like the one shown in fig. 4.2 are dominated by the infrared region. The renormalised light fermion insertions are given by

$$-\frac{2}{3}N_f \frac{\alpha_s}{4\pi} \left[\ln \left(\frac{-k^2}{\mu^2} \right) - \frac{5}{3} \right], \quad (10)$$

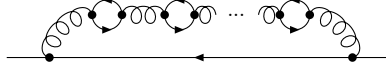


Figure 1 – Self-energy insertions on the gluon line leading to the renormalon ambiguity.

with k being the gluon momentum, which still needs to be integrated over. Due to the logarithm the ultraviolet and the infrared region are enhanced. A power series is Borel-summable if the Borel transform has no singularities on the real positive axis and does not increase too rapidly at positive infinity. With the replacement $\beta_{0,N_f} \rightarrow \beta_0$ one finds that the ultraviolet region leads to (non-critical) poles along the negative real axis, while the infrared region leads to poles along the positive real axis. Therefore this subset of diagrams is not Borel-summable and the full perturbative series can only be summed up to an infrared renormalon ambiguity. The renormalon ambiguity is of $\mathcal{O}(\Lambda_{\text{QCD}})^{21,22,23,24}$. This ambiguity limits the precision by which the pole mass can be extracted from experiment.

In perturbation theory one can convert between different different renormalisation schemes. We therefore have a relation between the $\overline{\text{MS}}$ -mass and the pole mass, which with the notation $\bar{m} = m_{\overline{\text{MS}}}(\mu = m_{\overline{\text{MS}}})$ reads

$$m_{\text{pole}} = \bar{m} \times \left[1 + c_1 \frac{\alpha_s(\bar{m})}{\pi} + c_2 \left(\frac{\alpha_s(\bar{m})}{\pi} \right)^2 + c_3 \left(\frac{\alpha_s(\bar{m})}{\pi} \right)^3 + c_4 \left(\frac{\alpha_s(\bar{m})}{\pi} \right)^4 + \dots \right]. \quad (11)$$

The coefficients are known to four-loop order, the last coefficient c_4 was computed quite recently^{25,26,27}. Numerically, we have for the top quark:

$$m_{\text{pole}} = \bar{m} \times [1 + 0.046 + 0.010 + 0.003 + 0.001 + \dots]. \quad (12)$$

The perturbative series appearing on the right-hand side of eq. (11) is again only an asymptotic series and has an renormalon ambiguity as well. This is clear from the fact that \bar{m} is free of renormalon ambiguities, while m_{pole} on the left-hand side suffers from a renormalon ambiguity.

Crude estimates of the renormalon ambiguity may be either obtained from renormalon-based calculations²², yielding

$$\delta m_{\text{pole}} \approx C_F \frac{2\pi}{\beta_0} e^{\frac{5}{6}} \Lambda_{\text{QCD}} \left(\ln \frac{\bar{m}^2}{\Lambda_{\text{QCD}}^2} \right)^{-\frac{\beta_1}{2\beta_0^2}} \approx \mathcal{O}(300 \text{ MeV}), \quad (13)$$

with $\beta_0 = 11 - 2N_f/3$ and $\beta_1 = 102 - 38N_f/3$, or from the last known term in the conversion formula in eq. (11). The latter gives

$$\delta m_{\text{pole}} \approx c_4 \bar{m} \left(\frac{\alpha_s(\bar{m})}{\pi} \right)^4 \approx \mathcal{O}(200 \text{ MeV}). \quad (14)$$

Let us stress that both numbers are just crude estimates. Let us also note that the spread of two (or more) ad-hoc non-perturbative models might not reflect the true uncertainty from non-perturbative effects.

Let us finally mention that the top width is not affected by a renormalon ambiguity, when expressed in terms of a short-distance mass^{21,24}.

4.3 The MSR-scheme

We have seen that the pole mass is ambiguous by an amount of order $\mathcal{O}(\Lambda_{\text{QCD}})$. But on the other hand the measurement of the peak position of the decay products of the top quark is an experimental observable. This brings us to the question, if one can translate a measurement

Table 1: Summary of the relevant scales, the appropriate effective theories together with the relevant matrix elements. Also indicated is the impact on the peak distribution and the dependence on the top mass.

Scale	Effective theory	Matrix elements	Impact on invariant mass distribution	Top mass dependence
$Q \dots m_t$	QCD	hard function	norm of the distribution	depends on m_t
$m_t \dots \Gamma_t$	SCET	jet function	shape and position	depends on m_t
$\Gamma_t \dots \Lambda_{QCD}$	top-HQET	soft function	shape and position	independent of m_t

of the peak position into a theoretical well defined short-distance mass. As experimentalists can measure many things to high precision (like for example the average number of pions in pp collisions), the question is if and how a measured quantity can be related to a quantity depending only on short-distance physics (the average number of pions is not a short-distance quantity). Before answering this question, let us analyse the problem in more detail. We should first find out, which scales are involved. In a second step we have to address the question on how to define a short-distance mass at a given scale. In the final step we then tackle the issue on how to translate the measurement into a short-distance mass.

Let us start with the involved scales. Effective theories are the appropriate tool to describe the relevant degrees of freedom at a given scale μ . Evolution operators allow us to move from a scale μ_1 to a scale μ_2 . The evolution operators sum up large logarithms and avoid in this way large logarithms, which may otherwise spoil a perturbative expansion. Applied to the top mass, this has been analysed in detail for top pair production in electron-positron annihilation^{28,29} and similar results are expected to hold for pp -collisions³⁰. The relevant scales are the centre-of-mass energy Q , the top mass m_t , the top width Γ_t and Λ_{QCD} . These scales are ordered as

$$\Lambda_{QCD} < \Gamma_t < m_t < Q. \quad (15)$$

In the range $[m_t, Q]$ physics is described by QCD, while in the range $[\Gamma_t, m_t]$ the appropriate description is in terms of soft-collinear effective theory (SCET). At even lower scales $[\Lambda_{QCD}, \Gamma_t]$ one uses a version of heavy quark effective theory adapted to top quarks (top-HQET). The relevant matrix elements for the various effective theories are the hard function, the jet function and the soft function, respectively. The impact on the invariant mass distribution from the various scales is as follows: Scales in the range $[\Gamma_t, m_t]$ affect mainly the norm of the distribution. The change in normalisation depends on m_t . Scales from the range $[\Gamma_t, m_t]$ have an impact on the shape and the position of the peak and these effects depend again on m_t . For the low scales from the range $[\Lambda_{QCD}, \Gamma_t]$ one finds that these scales influence as well the shape and the position of the peak. However it is important to note that those effects are independent of m_t . The situation is summarised in table 1. Since the effects from the scales $[\Lambda_{QCD}, \Gamma_t]$ are independent of m_t , it follows that we need a short-distance mass definition for scales down to Γ_t . The basic idea for the construction of an appropriate short-distance mass is to remove contributions which would give rise to the renormalon ambiguity. This approach is taken from experience with bottomium physics, where short-distance masses like the potential subtracted mass m_{PS} ³¹ or the 1S-mass m_{1S} ^{32,33} have been considered. For the top quark this will involve apart from the UV-renormalisation scale μ a second scale R . The \overline{MS} -mass is an example of a short-distance mass and we have $R = \bar{m}$ in this case. The MSR-mass³⁴ is a two-scale generalisation with a UV-scale μ and an IR-scale R , such that

$$m_{MSR}(R=0) = m_{pole}, \quad m_{MSR}(R=\bar{m}) = \bar{m}. \quad (16)$$

We may think of a short-distance mass definition in the same way as we think about an infrared-safe jet definition. A jet is defined by the specification of a jet algorithm (SIScone, k_t -algorithm,

anti- k_t -algorithm, etc.) and by a set of parameters associated to this algorithm ($R, f, n_{\text{pass}}, y_{\text{cut}},$ etc.). In the same way a short-distance mass is defined by the specification of a short-distance renormalisation scheme ($\overline{\text{MS}}$ -scheme, MSR-scheme, etc.) and by a set of parameters associated to this renormalisation scheme ($\mu, R,$ etc.).

As the soft function is independent of the top mass (and information on the soft function may be obtained from massless jet distributions), the peak position of the top invariant mass distribution can be related to a short-distance mass at a scale of Γ_t .

We now discuss how a measurement of the top invariant mass distribution can be translated into a short-distance mass. In the actual extraction of the top mass from experimental measurements theory sneaks in through the use of the template method or the matrix element method. For example, within the template method one generates first from Monte Carlo events for various values of m_{MC} and then determines the best fit to the experimental data. The Monte Carlo mass m_{MC} is only implicitly defined through the program code of the Monte Carlo. However, the factorisation of the effective field theory approach (hard function/jet function/soft function) has an analogy in typical event generators (hard matrix element/parton shower/hadronisation) and the shower cut-off scale is typically of the order of Γ_t (this is a numerical coincidence). Because the shower cut-off provides a strict infrared cut-off for long-distance effects, it can be argued that the Monte Carlo mass m_{MC} is something like a low-scale short-distance mass. Therefore a measurement based on the top invariant mass distribution determines the Monte Carlo mass m_{MC} , which is a short-distance mass defined implicitly through the program code of a specific Monte Carlo. In principle we could convert this mass to any other mass definition, but in the case at hand we are hampered by the fact that a precise definition of the Monte Carlo mass is not accessible. Parametrising the ignorance of a precise definition of the Monte Carlo mass, Hoang and Stewart³⁰ made in a contribution to the Top Quark Physics workshop in 2008 a first estimate for the translation to the MSR-mass:

$$m_{\text{MC}} = m_{\text{MSR}}(R = 1 \dots 9 \text{ GeV}). \quad (17)$$

The uncertainty in the infrared scale R introduces an uncertainty of the order of 1 GeV on the translation from the Monte Carlo mass to the MSR mass. Let us summarise: The Monte Carlo mass is a (not so well specified) short-distance mass and the translation from the Monte Carlo mass to a theoretically well defined short-distance mass at a low scale is currently estimated to be of the order of 1 GeV^{30,35}.

4.4 Work to do

There are ample opportunities to improve the current state of the art. They can be grouped into three categories.

First of all, the details related to factorisation and the various effective theories have only been worked out for $t\bar{t}$ -production in electron-positron annihilation. This remains to be done for pp -collisions. Although it is believed that the general picture will hold in pp -collisions as well, there are some modifications related to initial state partons and phase space cuts imposed by the jet algorithm. These issues were absent in the e^+e^- -analysis: There are no initial state partons and the analysis was based on hemisphere masses.

Secondly, it is worth studying the translation from the Monte Carlo mass to a well defined short-distance mass in more detail. In particular, one should firmly establish that the shower cut-off effectively implements some short-distance mass. In addition, the translation and the uncertainty from the Monte Carlo mass to a well defined short-distance mass can be improved.

Thirdly, it is worth a thought to envisage a dedicated event generator, based on a well defined short-distance top mass. This would eliminate the translation from a Monte Carlo mass to a well defined short-distance and the corresponding uncertainties from this part. This might not be impossible. In fact, there are proposals in the literature in a context not specific to top physics to go from effective theories like SCET to exclusive event generators^{36,37,38}.

5 Conclusions

The precise numerical value of the top mass is essential for many analyses in high-energy precision physics. With the ongoing LHC experiments the error on the top mass is approaching $\mathcal{O}(\Lambda_{\text{QCD}})$. At this precision, an adequate short-distance mass definition is mandatory. The pole mass is not a short-distance mass and ambiguous by an amount of $\mathcal{O}(\Lambda_{\text{QCD}})$. The $\overline{\text{MS}}$ -mass is a short-distance mass and can be used at high scales. The MSR-mass is a generalisation of the $\overline{\text{MS}}$ -mass and can also be used as a short-distance mass at lower scales.

As an outlook towards the future it is expected that a threshold scan at an e^+e^- -machine will be able to determine the top quark mass with a precision below 100 MeV. Again, the use of an adequate short-distance mass like the potential subtracted mass or the 1S-mass is mandatory.

References

1. CDF, F. Abe *et al.*, Phys.Rev.Lett. **74**, 2626 (1995), arXiv:hep-ex/9503002.
2. D0, S. Abachi *et al.*, Phys.Rev.Lett. **74**, 2632 (1995), arXiv:hep-ex/9503003.
3. Particle Data Group, K. Olive *et al.*, Chin.Phys. **C38**, 090001 (2014).
4. ATLAS, CDF, CMS, D0, (2014), arXiv:1403.4427.
5. U. Langenfeld, S. Moch, and P. Uwer, Phys. Rev. **D80**, 054009 (2009), arXiv:0906.5273.
6. M. Dowling and S.-O. Moch, Eur.Phys.J. **C74**, 3167 (2014), arXiv:1305.6422.
7. M. Czakon, P. Fiedler, and A. Mitov, Phys.Rev.Lett. **110**, 252004 (2013), arXiv:1303.6254.
8. S. Moch and P. Uwer, Phys. Rev. **D78**, 034003 (2008), arXiv:0804.1476.
9. M. Czakon, A. Mitov, and G. F. Sterman, Phys. Rev. **D80**, 074017 (2009), arXiv:0907.1790.
10. M. Cacciari, M. Czakon, M. Mangano, A. Mitov, and P. Nason, Phys.Lett. **B710**, 612 (2012), arXiv:1111.5869.
11. N. Kidonakis, Phys. Rev. **D82**, 114030 (2010), arXiv:1009.4935.
12. V. Ahrens, A. Ferroglia, M. Neubert, B. D. Pecjak, and L. L. Yang, JHEP **09**, 097 (2010), arXiv:1003.5827.
13. M. Beneke, P. Falgari, S. Klein, and C. Schwinn, Nucl. Phys. **B855**, 695 (2012), arXiv:1109.1536.
14. A. Denner, S. Dittmaier, S. Kallweit, and S. Pozzorini, Phys. Rev. Lett. **106**, 052001 (2011), arXiv:1012.3975.
15. G. Bevilacqua, M. Czakon, A. van Hameren, C. G. Papadopoulos, and M. Worek, JHEP **02**, 083 (2011), arXiv:1012.4230.
16. S. Dittmaier, P. Uwer, and S. Weinzierl, Phys. Rev. Lett. **98**, 262002 (2007), hep-ph/0703120.
17. S. Dittmaier, P. Uwer, and S. Weinzierl, Eur. Phys. J. **C59**, 625 (2009), arXiv:0810.0452.
18. K. Melnikov and M. Schulze, Nucl. Phys. **B840**, 129 (2010), arXiv:1004.3284.
19. K. Melnikov, A. Scharf, and M. Schulze, Phys.Rev. **D85**, 054002 (2012), arXiv:1111.4991.
20. S. Alioli *et al.*, Eur.Phys.J. **C73**, 2438 (2013), arXiv:1303.6415.
21. I. I. Y. Bigi, M. A. Shifman, N. G. Uraltsev, and A. I. Vainshtein, Phys. Rev. **D50**, 2234 (1994), arXiv:hep-ph/9402360.
22. M. Beneke and V. M. Braun, Nucl.Phys. **B426**, 301 (1994), arXiv:hep-ph/9402364.
23. M. Beneke, Phys. Lett. **B344**, 341 (1995), arXiv:hep-ph/9408380.
24. M. C. Smith and S. S. Willenbrock, Phys. Rev. Lett. **79**, 3825 (1997), arXiv:hep-ph/9612329.
25. K. Chetyrkin and M. Steinhauser, Nucl.Phys. **B573**, 617 (2000), arXiv:hep-ph/9911434.
26. K. Melnikov and T. v. Ritbergen, Phys.Lett. **B482**, 99 (2000), arXiv:hep-ph/9912391.
27. P. Marquard, A. V. Smirnov, V. A. Smirnov, and M. Steinhauser, Phys.Rev.Lett. **114**, 142002 (2015), arXiv:1502.01030.

- 28. S. Fleming, A. H. Hoang, S. Mantry, and I. W. Stewart, Phys. Rev. **D77**, 074010 (2008), arXiv:hep-ph/0703207.
- 29. S. Fleming, A. H. Hoang, S. Mantry, and I. W. Stewart, Phys.Rev. **D77**, 114003 (2008), arXiv:0711.2079.
- 30. A. H. Hoang and I. W. Stewart, Nucl.Phys.Proc.Suppl. **185**, 220 (2008), arXiv:0808.0222.
- 31. M. Beneke, Phys.Lett. **B434**, 115 (1998), arXiv:hep-ph/9804241.
- 32. A. H. Hoang, Z. Ligeti, and A. V. Manohar, Phys.Rev. **D59**, 074017 (1999), arXiv:hep-ph/9811239.
- 33. A. Hoang and T. Teubner, Phys.Rev. **D60**, 114027 (1999), arXiv:hep-ph/9904468.
- 34. A. H. Hoang, A. Jain, I. Scimemi, and I. W. Stewart, Phys.Rev.Lett. **101**, 151602 (2008), arXiv:0803.4214.
- 35. S. Moch *et al.*, (2014), arXiv:1405.4781.
- 36. C. W. Bauer and M. D. Schwartz, Phys.Rev. **D76**, 074004 (2007), arXiv:hep-ph/0607296.
- 37. C. W. Bauer, F. J. Tackmann, and J. Thaler, JHEP **12**, 010 (2008), arXiv:0801.4026.
- 38. C. W. Bauer, F. J. Tackmann, and J. Thaler, JHEP **12**, 011 (2008), arXiv:0801.4028.